

Expression of epithelial-mesenchymal transition regulators SNAI2 and TWIST1 in thyroid carcinomas

Darya Buehler¹, Heather Hardin¹, Weihua Shan¹, Celina Montemayor-Garcia¹,
Patrick S Rush¹, Sofia Asioli², Herbert Chen³ and Ricardo V Lloyd¹

¹Department of Pathology and Laboratory Medicine, University of Wisconsin School of Medicine and Public Health, K4/436 Clinical Science Center, Madison, WI, USA; ²Department of Biomedical Sciences and Human Oncology, University of Turin, Turin, Italy and ³Department of Surgery, University of Wisconsin School of Medicine and Public Health, Madison, WI, USA

Epithelial–mesenchymal transition is an important mechanism of epithelial tumor progression, local invasion and metastasis. The E-cadherin (CDH1) repressor SLUG (SNAI2) and the basic helix–loop–helix transcription factor TWIST1 inhibit CDH1 expression in poorly differentiated malignancies as inducers of epithelial–mesenchymal transition. Epithelial–mesenchymal transition has been implicated in progression from well to poorly differentiated/anaplastic thyroid carcinoma but the expression of SNAI2 and TWIST1 proteins and their phenotypic association in human thyroid cancers has not been extensively studied. We examined the expression of SNAI2, TWIST1 and CDH1 by immunohistochemistry in a panel of well-differentiated and anaplastic thyroid cancers and by qRT-PCR in thyroid cell lines. Ten normal thyroids, 33 follicular adenomas, 56 papillary thyroid carcinomas including 28 follicular variants, 27 follicular carcinomas and 10 anaplastic thyroid carcinomas were assembled on a tissue microarray and immunostained for SNAI2, TWIST1 and CDH1. Most (8/10) anaplastic thyroid carcinomas demonstrated strong nuclear immunoreactivity for SNAI2 with associated absence of CDH1 in 6/8 cases (75%). TWIST1 was expressed in 5/10 anaplastic thyroid carcinomas with absence of CDH1 in 3/5 (60%) cases. These findings were confirmed in whole sections of all anaplastic thyroid carcinomas and in a separate validation set of 10 additional anaplastic thyroid carcinomas. All normal thyroids, follicular adenomas, papillary and follicular thyroid carcinomas were negative for SNAI2 and TWIST1 ($P < 0.0001$) and all showed strong diffuse immunoreactivity for CDH1 ($P = 0.026$). Expression of SNAI2, TWIST1 and CDH1 mRNA varied in a normal thyroid, papillary carcinoma and two anaplastic thyroid carcinoma cell lines tested, but the highest levels of CDH1 mRNA were detected in the normal thyroid cell line while the anaplastic thyroid carcinoma cell line demonstrated the highest levels of SNAI2 and TWIST1 mRNA. Our findings support the role of epithelial–mesenchymal transition in the development of anaplastic thyroid carcinoma.

Modern Pathology (2013) **26**, 54–61; doi:10.1038/modpathol.2012.137; published online 17 August 2012

Keywords: anaplastic thyroid carcinoma; CDH1; SNAI2; thyroid carcinoma; thyroid cell lines; TWIST1

Epithelial–mesenchymal transition is now commonly accepted as a key pathologic mechanism in epithelial tumor progression, local invasion, metastasis and therapeutic resistance, and is linked

Correspondence: Dr RV Lloyd, MD, PhD, Department of Pathology and Laboratory Medicine, University of Wisconsin School of Medicine and Public Health, K4/436 Clinical Science Center, Box 8550, 600 Highland Avenue, Madison, WI 53792, USA.

E-mail: rvlloyd@wisc.edu

This work was presented in part at the 101st United States and Canadian Academy of Pathology Annual Meeting, Vancouver, BC, Canada, 17 March 2012–23 March 2012.

Received 17 May 2012; revised 9 July 2012; accepted 10 July 2012; published online 17 August 2012

to acquisition of stem-like properties by cancer cells.^{1–3} The hallmark of epithelial–mesenchymal transition is loss of E-cadherin (CDH1) expression due to the activation of several epithelial–mesenchymal transition inducers including E-cadherin repressors SNAI1 (SNAIL), SNAI2 (SLUG) and ZEB and the basic helix–loop–helix transcription factor TWIST1.^{1,4} This in turn leads to loss of cellular adhesion and polarity and acquisition of migratory and invasive phenotype by epithelial cells. A growing body of evidence has shown upregulation of SNAI1, SNAI2 and TWIST1 in a broad spectrum of human malignancies. This has been associated with aggressive tumor behavior and poor prognosis.^{5–9}

Recent studies in thyroid tumors have supported a role of epithelial–mesenchymal transition in thyroid carcinogenesis. Vasco *et al*¹⁰ using gene expression profiling and confirmatory functional studies in papillary thyroid carcinoma, demonstrated upregulation of epithelial–mesenchymal transition-related genes at the invasive edge but not in the central portion of papillary thyroid carcinomas. The authors also showed that overexpression of vimentin, a marker of epithelial–mesenchymal transition-like phenotype in papillary thyroid carcinoma, was associated with tumor invasiveness, multifocality and lymph node metastasis. Epithelial–mesenchymal transition has also been implicated in the development of anaplastic thyroid carcinoma, a highly aggressive malignancy with mesenchymal morphology and poor prognosis.¹¹ Frequent loss of CDH1 expression has been reported in anaplastic thyroid carcinoma, consistent with the epithelial–mesenchymal transition-like phenotype.^{12–15} Epithelial–mesenchymal transition occurred during progression of BRAF-induced papillary thyroid carcinoma to poorly differentiated/undifferentiated thyroid carcinoma in a mouse model.¹⁵ Recently, Salerno *et al*¹⁶ showed functionally relevant upregulation of TWIST1 in anaplastic thyroid carcinoma cell line, further supporting the role of epithelial–mesenchymal transition in the pathogenesis of this aggressive malignancy. Despite the ample functional evidence for the role of epithelial–mesenchymal transition in thyroid cancer, the data on the expression of SNAI1, SNAI2 and TWIST1 and their phenotypic association in human thyroid tumor samples is rather limited. Hardy *et al*¹⁷ demonstrated expression of epithelial–mesenchymal transition regulators SNAI1 and SNAI2 by immunohistochemistry in approximately half of the follicular thyroid carcinomas and 87% of papillary thyroid carcinomas. In contrast, Salerno *et al*¹⁶ reported that another epithelial–mesenchymal transition marker, Twist, was detected by immunohistochemistry only in human anaplastic thyroid carcinomas (49%) but not in well-differentiated or poorly differentiated thyroid cancers. To better understand the correlation between the expression of epithelial–mesenchymal transition markers and the morphologic phenotype, we examined the expression of SNAI2, TWIST1 and CDH1 by immunohistochemistry in a panel of 146 human thyroid tissues/tumors and by RT-PCR in thyroid cell lines.

Materials and methods

Patients

The study was approved by the Institutional Review Board. Patients diagnosed with follicular adenoma, follicular thyroid carcinoma, papillary thyroid carcinoma (including follicular variant) and anaplastic thyroid carcinoma were identified using a surgical

pathology database. Corresponding hematoxylin and eosin-stained slides were reviewed for confirmation of the diagnosis. Clinical records were accessed for the following information: sex and age at diagnosis, family and personal history of thyroid disease, history of radiation exposure/therapy, clinical and/or radiologic evidence of lymph node or systemic metastases and the date of last follow-up or death. Data on the tumor size, multifocality, histologic type, and the presence of vascular invasion and lymph node metastases was extracted from the surgical pathology reports. Follow-up time was calculated as months between the date of the diagnosis and the date of the last follow-up. Patients were considered to be lost to follow-up if no medical information was obtainable beyond the original surgery.

Construction of the tissue microarray. After confirmation of the diagnosis, the most representative areas of the formalin-fixed paraffin-embedded thyroid tumors were assembled on a tissue microarray in triplicate 0.6 mm cores using manual tissue microarrayer (Beecher Instruments, Sun Prairie, WI, USA). For normal thyroid controls, we used thyroid tissue incidentally removed from patients undergoing surgery for hyperparathyroidism or the opposite (histologically normal) thyroid lobe in patients with follicular or papillary carcinoma. Sections of 5 µm were cut for subsequent immunohistochemical analysis. The placement of the tissue cores on the recipient block of the microarray was confirmed by the hematoxylin and eosin stain.

Validation set. An additional 10 cases of whole tissue sections of anaplastic thyroid carcinoma were used to validate the findings from the tissue microarray.

Cell lines. The normal thyroid cell line NTHY-ORI 3-1 was purchased from Sigma Chemical (St Louis, MO, USA). TPC-1 was kindly provided by Dr H. Chen (Department of Surgery, University of Wisconsin-Madison, WI, USA). Both cell lines were maintained in RPMI and 10% FBS plus 1% penicillin/streptomycin at 37 °C, 5% CO₂. The THJ-16T and THJ-21T cell lines were kindly provided by Dr J. Copland (Department of Cancer Biology, Mayo Clinic, Jacksonville, FL, USA) and maintained in RPMI with 10% FBS, 1% non-essential amino acids, 1% sodium pyruvate and 1% penicillin/streptomycin at 37 °C, 5% CO₂.

RNA isolation and quantitative RT-PCR. Total RNA was isolated with TRIzol Reagent (Invitrogen, Grand Island, NY, USA) according to manufacturer's instructions. RNA quality and concentration were assessed on the NanoDrop 1000 (Thermo Scientific, Pittsburgh PA, USA). Total RNA of 1 µg was reverse transcribed using the All-In-One First-Strand cDNA Synthesis Kit (GeneCopoeia, Rockville, MD, USA) with Oligo(dT) primer. PCR primers used were as

follows: ECAD forward 5'-CCAGGAACCTCTGTGAT GGA-3' and ECAD reverse 5'-TTTGTCAAGGGAGCT CAGGA-3', TWIST forward 5'-AGCTACGCCTCT CGGTCT-3' and TWIST reverse 5'-CCTTCTCTGGAA ACAATGACATC-3', SLUG forward 5'-TTCAAGG ACACATTAGAACTCACAC-3' and SLUG reverse 5'-TCTTACATCAGAATGGGTCTGC-3' and 18S forward 5'-GTAACCCGTTGAACCCCATT-3' and 18S reverse 5'-CCATCCAATCGGTAGTAGCG-3'. The qRT-PCR was performed on the CFX96 PCR detection system (Bio-Rad, Hercules, CA, USA). Relative quantities determined by the delta-delta CT method.

Immunohistochemistry. For automated immunostaining, 5 µm thick tissue microarray sections were deparaffinized followed by heat-induced epitope retrieval using the Lab Vision PT module (Thermo Scientific) with Lab Vision citrate buffer pH 6.0. All immunolabeling was performed at room temperature using the Lab Vision 360 LV-1 Autostainer system (Thermo Scientific). All reagents used were from Biocare Medical, Chicago II, USA, except where noted. Endogenous peroxidase was blocked for 5 min with Peroxidized-1. Nonspecific protein binding was blocked by Sniper and nonspecific avidin was blocked using the Avidin-Biotin kit, incubating 15 min for each reagent. Antibodies to CDH1 (Cell SignalingTechnology, Beverly, MA, USA, clone 24E10, 1:400), SNAI2 (Cell Signaling, clone C1967, 1:100) and Twist1 (Abcam, Cambridge, MA, USA, polyclonal, 1:250) were incubated for 60 min followed by incubation with biotinylated goat anti-mouse IgG for 15 min and subsequent 4plus Streptavidin-HRP treatment for 15 min. Beta-zoid Diaminobenzidine and Mayer's Hematoxylin were each incubated for 1 min. Primary antibodies were omitted in negative controls, which resulted in no staining. For positive controls, thyroid tumors previously shown to express the antigen of interest by immunohistochemistry and by RT-PCR were used. For manual immunostaining, full tissue sections of the anaplastic thyroid carcinomas were deparaffinized followed by microwave heat-induced epitope retrieval with 10 mM citrate buffer pH 6 for 20 min. Endogenous peroxidase was blocked with 3% hydrogen peroxide for 15 min followed by a

nonspecific protein block with a 2.5% normal horse serum for 30 min. The above-mentioned primary antibodies were incubated overnight at 4 °C at half the dilution used for automated immunostaining. The following day the slides were washed and incubated for 30 min with the ImmPRESS Universal Peroxidase Reagent Kit (Vector Laboratories, Burlingame, CA, USA) and developed with the ImmPACT DAB Kit (Vector Laboratories) and Gills Hematoxylin (Vector Laboratories) incubating each for 1 min.

The immunohistochemistry scoring was performed by two independent observers (D.B. and R.V.L.) using conventional bright field microscopy and differences in interpretation were reviewed for consensus. Unequivocal nuclear staining pattern for SNAI2 and TWIST1 and membranous staining for CDH1 were interpreted based on the intensity as negative, weak (1+), moderate (2+) and strong (3+). Only 2+ and 3+ intensity of staining was considered to be positive. The expression was considered focal-positive cells comprised of 2–25% of all tumor cells in the tissue microarray sample and diffuse if this ratio was >25%. Focal staining of <1% of all tumor cells was considered to be negative.

Statistical analysis. Categorical variables were assessed using χ^2 , or with Fisher's exact test. Numerical variables were compared with one-way ANOVA. The statistical comparisons were performed using R software¹⁸ or GraphPad Prism version 5 software (San Diego, CA, USA).

Results

Clinicopathologic Characteristics and Outcomes

The patient's demographics and tumor characteristics of cases represented on the tissue microarray are presented in Table 1. One hundred and thirty six cases were evaluated including 33 cases of follicular adenoma, 28 cases of papillary thyroid carcinoma including 2 tall cell variants, 28 cases of follicular variant of papillary thyroid carcinoma, 27 cases of follicular thyroid carcinoma and 10 cases of anaplastic thyroid carcinoma. There was a female

Table 1 Patient and tumor characteristics of the thyroid tumor cases

Characteristics	Follicular adenoma	Papillary thyroid carcinoma	Follicular variant of papillary thyroid carcinoma	Follicular thyroid carcinoma	Anaplastic thyroid carcinoma
Number of cases	33	28	28	27	10
Gender	9 M/24 F	7 M/21 F	8 M/20 F	11 M/16 F	4 M/6 F
Age, median (range)	48 (16–77)	51 (14–83)	47 (25–76)	56 (18–83)	74 (60–86)
Family history of thyroid disease (%)	7 (21)	5 (18)	5 (18)	6 (22)	2 (20)
History of radiation exposure (%)	2 (6)	2 (7.1)	1 (3.6)	3 (11)	1 (10)
Size (mean, s.d.), mm	34.1 ± 14.7	23.8 ± 14.6	23.6 ± 13	44.3 ± 22.5	51.2 ± 36.1
Lymph node metastases (%)	0	14 (50)	5 (17.8)	3 (11)	1 (10)
Systemic metastases (%)	0	1 (3.6)	0	6 (22)	4 (40)

predominance in each group. As expected, the anaplastic thyroid carcinoma patients were significantly older (mean age of 74-year old at diagnosis) than patients with follicular adenomas and well-differentiated thyroid carcinomas. Family history of thyroid disease was identified in approximately 20% of patients in each group. The number of cases associated with a history of radiation exposure/treatment did not exceed 10% in any group. Mean tumor size was significantly higher in the follicular and the anaplastic thyroid carcinoma groups ($P<0.0001$, two-tailed one-way ANOVA). Thirteen (48%) of follicular thyroid carcinomas displayed features consistent with oxyphilic (Hurthle cell variant). In four patients with anaplastic thyroid carcinoma, the tumor appeared to have developed in a background of well-differentiated thyroid cancer (two follicular thyroid carcinomas, one oxyphilic carcinoma and one tall cell variant of papillary thyroid carcinomas). Lymph node metastases occurred in half of the patients with papillary thyroid carcinoma, 17.8% of patients with follicular variant of papillary thyroid carcinoma, 11% of patients with follicular thyroid carcinoma and in one (10%) patient with anaplastic thyroid carcinoma. Systemic metastases developed in 3.6% of patients with papillary, 22% of patients with follicular and 40% of patients with anaplastic thyroid carcinoma.

The patient's outcomes are presented in Table 2. The median follow-up was 36 months in patients with papillary thyroid carcinoma, 28.5 months in patients with follicular variant of papillary thyroid carcinoma, 46.5 months in patients with follicular thyroid carcinoma and 6 months in patients with anaplastic thyroid carcinoma. As expected, the most favorable clinical outcomes were observed in patients with papillary thyroid carcinoma, including the follicular variant, whereas more aggressive tumor behavior were observed in patients with anaplastic thyroid carcinoma.

Immunohistochemistry

Immunostaining for SNAI2, TWIST1 and CDH1 was performed in 136 formalin-fixed paraffin-embedded

samples of thyroid tissues/tumors assembled on a tissue microarray. Unequivocal nuclear immunoreactivity for SNAI2 and TWIST1 and membranous staining for CDH1 were analyzed as described in the Materials and Methods section. Moderate or strong (focal or diffuse) immunoreactivity was considered positive. Examples of immunohistochemical staining in papillary, follicular and anaplastic thyroid carcinoma along with the corresponding hematoxylin and eosin stain are demonstrated in Figure 1 and the summary of immunohistochemistry results in the entire cohort are presented in Table 3. Most (8/10) anaplastic thyroid carcinomas demonstrated strong nuclear immunoreactivity for SNAI2 (6 diffuse, 2 focal). In 6/8 cases (75%) of anaplastic thyroid carcinomas, expression of SNAI2 correlated with complete absence of CDH1 immunoreactivity. TWIST1 was detected in 5/10 anaplastic thyroid carcinomas with absence of CDH1 in 3/5 (60%) of these cases. SNAI2 and TWIST1 were undetectable in any of the normal thyroids, follicular adenomas, papillary thyroid carcinomas including tall cell and follicular variants, or follicular carcinomas ($P<0.00001$ for each protein, two-tailed Fisher's exact test). All normal thyroids, follicular adenomas and well-differentiated thyroid cancers showed strong diffuse immunoreactivity for CDH1 ($P=0.026$, two-tailed χ^2), including all lesions with Hurthle cell morphology. No difference in expression of SNAI2, TWIST1 and CDH1 was observed in papillary thyroid carcinomas with potentially more aggressive behavior including two tall cell variants and 20 conventional papillary carcinomas with invasive growth pattern. Immunoreactivity for SNAI2 and TWIST1 was also detected in the nuclei of stromal fibroblasts, endothelial cells and occasional inflammatory cells (not shown). To validate the tissue microarray findings, we repeated the immunostaining for SNAI2, TWIST1 and CDH1 in whole sections of all anaplastic thyroid carcinomas. The results in the anaplastic thyroid carcinoma closely matched the tissue microarray findings with regard to expression of SNAI2 and CDH1 (8/10 cases expressed SNAI2, 3/10 cases maintained CDH1); one additional case was found to diffusely express TWIST1 in the large

Table 2 Clinical outcomes

Disease status	Follicular adenoma	Papillary thyroid carcinoma	Follicular variant of papillary thyroid carcinoma	Follicular thyroid carcinoma	Anaplastic thyroid carcinoma
Alive without disease	33	22	23	15	2
Alive with disease	0	3	1	3	0
Died of disease	0	0	0	5	5
Died, no evidence of disease	0	0	0	1	2
Lost to follow-up	0	3	4	3	1
Total	33	28	28	27	10

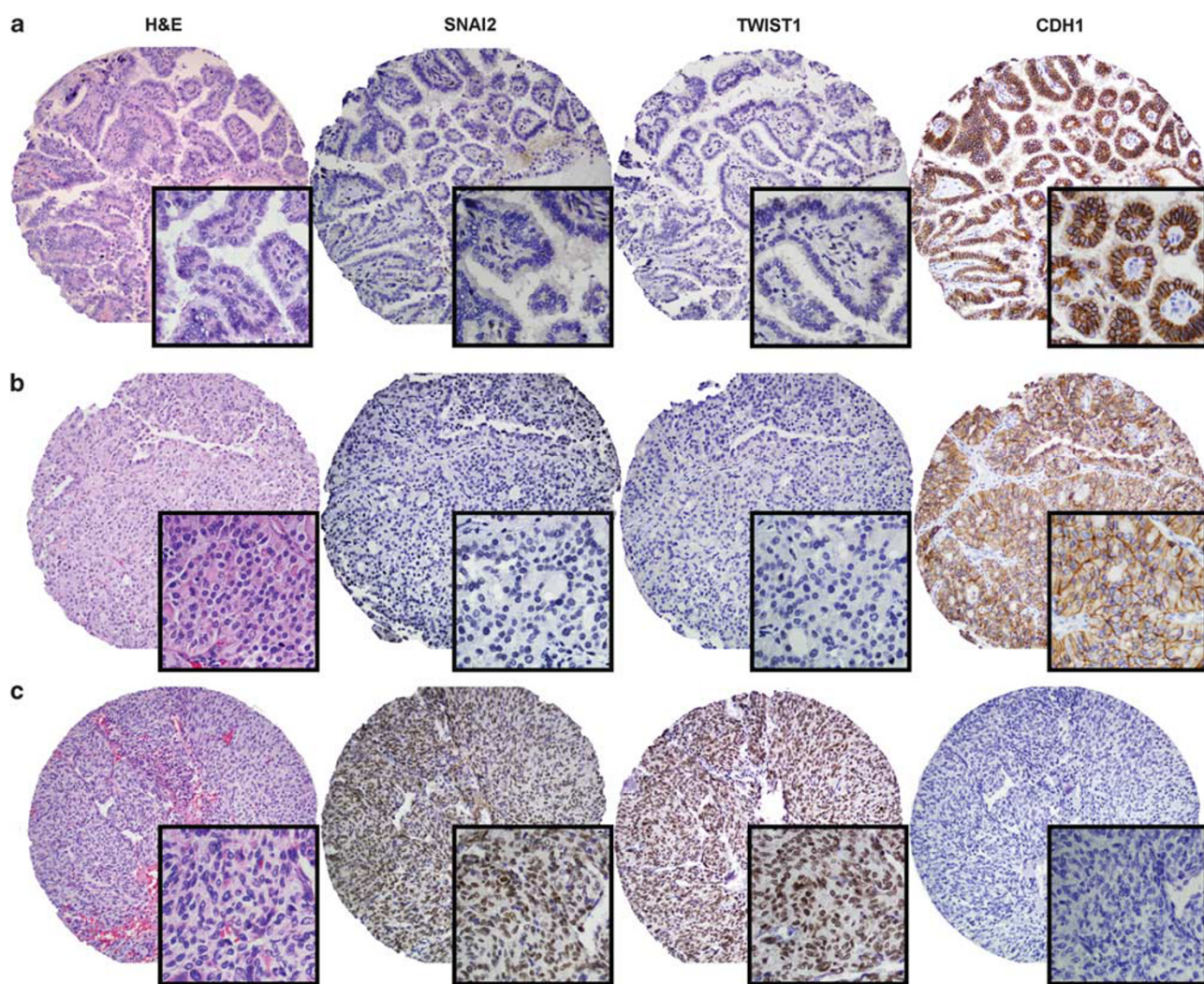


Figure 1 Examples of SNAI2, TWIST1 and CDH1 immunolabeling in (a) papillary thyroid carcinoma, (b) follicular thyroid carcinoma and (c) anaplastic thyroid carcinoma. Strong diffuse nuclear staining for SNAI2 and TWIST1 is observed in anaplastic thyroid carcinoma accompanied by loss of membranous staining for CDH1. The patient died in less than a month after the diagnosis. Papillary thyroid carcinoma and follicular thyroid carcinoma are positive for CDH1, but negative for SNAI2 and TWIST1.

Table 3 Expression of SNAI2, TWIST1 and CDH1 in thyroid tumors by immunohistochemistry (positive/total cases)

Antibody/tumor type	Normal thyroid	Follicular adenoma	Papillary thyroid carcinoma	Follicular variant of thyroid carcinoma	Follicular thyroid carcinoma	Anaplastic thyroid carcinoma
SNAI2 ^a	0/10	0/33	0/28	0/28	0/27	8/10 Diffuse 6/8 Focal 2/8
TWIST1 ^a	0/10	0/33	0/28	0/28	0/27	5/10 All diffuse
CDH1 ^b	10/10	33/33	28/28	28/28	27/27	3/10 (30%) All diffuse

^aTwo-tailed χ^2 , $P < 0.0001$.

^bTwo-tailed Fisher's exact test, $P = 0.026$.

section, which was focally positive for TWIST1 in the tissue microarray.

An additional 10 cases of whole sections of anaplastic thyroid carcinoma was used as a validation set. All of the patients died of disease within 14

months after the diagnosis. SNAI2 was positive in all 10 cases (100%), whereas TWIST1 was positive in 7 cases (70%). CDH1 was negative in all 10 cases.

To correlate the immunohistochemistry results with the morphologic appearance, the anaplastic

thyroid carcinomas were divided into predominantly epithelioid (11/20) and predominantly spindled (9/10) type. We did not observe an apparent correlation between the morphologic phenotype and expression of SNAI2, TWIST1 and CDH1 by immunohistochemistry. Correlation of SNAI2, TWIST1 and CDH1 expression with the tumor behavior in anaplastic thyroid carcinoma showed that all patients with known metastatic disease and all patients who died of disease by the cutoff time point had strong diffuse expression of SNAI2 and TWIST1 in their anaplastic thyroid carcinoma samples. There was no apparent relationship between loss of E-cadherin expression and disease outcome.

qRT-PCR in Thyroid Cell Lines

Expression of *SNAI2*, *TWIST1* and *CDH1* genes was examined at the level of mRNA in normal thyroid cell line NTHY-ORI 3-1, papillary cancer cell line TPC-1 and the THJ-16T and THJ-21T anaplastic thyroid carcinoma cell lines. The results are shown in Figure 2. Overall, the expression of SNAI2 and TWIST1 mRNAs in thyroid tumors was variable. However, the highest levels of CDH1 mRNA were detected in the normal thyroid cell line, which also showed no detectable SNAI2 and TWIST1 mRNA. In contrast, the 21T anaplastic thyroid carcinoma cell line demonstrated the highest levels of SNAI2 and TWIST1 mRNA and lower CDH1 mRNA expression levels relative to the normal thyroid cell line. Interestingly, the E-cadherin mRNA was not detected in PTC cell line TPC-1, which also showed low levels of SNAI2 and TWIST1 mRNA.

Discussion

Although the evidence supporting the role of epithelial–mesenchymal transition in thyroid carcinogenesis is increasing, the data on the expression of the specific mediators of this process such as

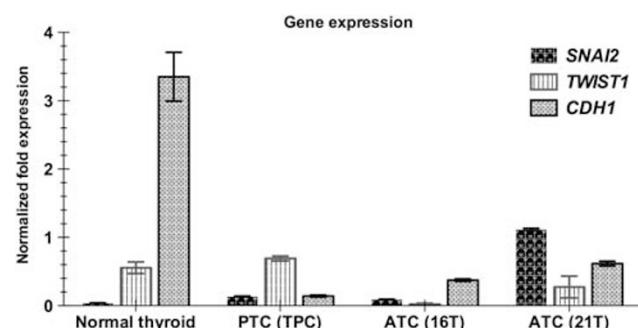


Figure 2 Expression of SNAI2, TWIST1 and CDH1 mRNA in the normal thyroid, papillary thyroid carcinoma and anaplastic thyroid carcinoma cell lines by qRT-PCR. The highest levels of CDH1 mRNA were detected in the normal thyroid cell line while the T21 anaplastic thyroid carcinoma cell line demonstrated the highest levels of SNAI2 and TWIST1 mRNA.

SNAI1, SNAI2 and TWIST1 and their phenotypic association in human thyroid carcinoma samples are limited. In the present study, we have demonstrated strong diffuse expression of SNAI2 and TWIST1 by immunohistochemistry and concomitant loss of CDH1 expression in the majority of anaplastic thyroid carcinomas but not in normal thyroids, thyroid adenomas or well-differentiated thyroid carcinomas. Our findings with TWIST1 are in agreement with the previous study by Salerno *et al*¹⁶ who reported expression of TWIST1 by immunohistochemistry only in human anaplastic thyroid carcinoma samples but are in contrast to earlier observations by Hardy *et al*¹⁷ who detected epithelial–mesenchymal transition inducers SNAI1 and SNAI2 by immunohistochemistry in about half of the follicular thyroid carcinomas and in a substantial proportion (87%) of papillary thyroid carcinomas. Possible reasons for the lack of SNAI2 expression or reduction in CDH1 staining in our papillary thyroid carcinoma samples include the use of different antibodies or occurrence of epithelial–mesenchymal transition at the invasive front but not in the central portion of the papillary thyroid carcinoma as demonstrated by Vasco *et al*¹⁰ and Riesco–Eizaguirre *et al*,¹⁹ and the invasive edge of the tumor was less likely to be represented on the tissue microarray. However, we did not detect SNAI2 or TWIST1 immunoreactivity or a difference in CDH1 expression by immunohistochemistry between the central area and the invasive edge in five randomly selected whole sections of invasive papillary thyroid carcinoma included in the tissue microarray (data not shown).

Our observations of inverse relationship between expression of epithelial–mesenchymal transition inducers SNAI2, TWIST1 and CDH1 in the majority of human anaplastic thyroid carcinoma samples agree with the recent functional *in vitro* and *in vivo* studies supporting the unique role of epithelial–mesenchymal transition in the development of this very aggressive malignancy. Knauf *et al*^{15,19} showed activation of the EMT regulators SNAI1, ZEB1 and ZEB2 with concurrent alterations in CDH1 expression during progression from BRAF-mutated papillary thyroid carcinoma to undifferentiated carcinoma in mice, likely due to the activation of TGF beta/SMAD pathway. Dereulation of the epithelial–mesenchymal transition suppressor miR-200 family and concomitant upregulation of the inducers ZEB1 and ZEB2 has been demonstrated in anaplastic thyroid carcinoma, but not in well-differentiated thyroid cancers.¹⁴ Using functional *in vitro* studies, Salerno *et al*¹⁶ proposed that TWIST1 may have diverse roles in anaplastic and in papillary thyroid carcinoma cell lines, including induction of epithelial–mesenchymal transition and promoting mesenchymal phenotype as well as an antiapoptotic effect. Cancer stem cell-like properties have been recently demonstrated in cell lines and human samples of anaplastic thyroid carcinoma.^{20,21} A recent

immunohistochemical study suggested that cancer stem cell-like properties in anaplastic thyroid carcinoma also display attributes of epithelial-mesenchymal transition.²²

Understanding the relationship between the expression of epithelial-mesenchymal transition proteins and morphologic phenotype in anaplastic thyroid carcinoma has been problematic due to very low number of cases in most studies and lack of agreement on how to subtype these cancers by morphology in general. Salerno *et al*¹⁶ reported a significant inverse correlation between expression of TWIST1 by immunohistochemistry and epithelioid morphology in anaplastic thyroid carcinoma. Similarly, Knauf *et al*¹⁵ suggested a correlation between squamoid vs mesenchymal morphology and the presence or absence of membranous E-cadherin staining in anaplastic thyroid carcinoma. Both the authors speculate that immunohistochemical detection of epithelial-mesenchymal transition in anaplastic thyroid carcinoma correlates with the mesenchymal phenotype. Possible molecular events related to the acquisition of mesenchymal features induced by epithelial-mesenchymal transition in thyroid carcinoma have been explored in recent studies. Vasco *et al*¹⁰ showed downregulation of genes involved in cell-cell adhesion and communication at the level of mRNA and overexpression of RUNX2 and fibronectin by immunohistochemistry at the invasive front of papillary thyroid carcinomas characterized by epithelial-mesenchymal transition. In the mouse model of progression from *BRAF*-mutated papillary thyroid carcinoma to undifferentiated carcinoma,¹⁵ expression of inducers of epithelial-mesenchymal transition SNAI1, ZEB1 and ZEB2 was associated with significant downregulation of genes involved in tight junctions, desmosomes and adherent junction proteins and upregulation of intermediate filaments and basement membrane genes. These findings correlated at the morphologic level with spindle cell morphology and loss of E-cadherin and expression of vimentin immunostain by immunohistochemistry. We did not find an association between epithelioid or spindle cell morphology and SNAI2, TWIST1 and CDH1 expression in our anaplastic thyroid carcinoma samples, although this assessment was based on morphology and did not include immunostaining for vimentin.

A positive correlation between the expression of epithelial-mesenchymal transition inducers SNAI1, SNAI2 and TWIST1 in the tumor cells and in cancer-associated fibroblasts, and aggressive tumor behavior has been suggested in a variety of human malignancies including breast, endometrial, ovarian, colon, gastric and other cancers.^{5-8,23} One exception is a recent analysis of SNAI1 and SNAI2 expression in renal cell carcinoma.⁹ The authors found that SNAI2-positive renal cell carcinoma was associated with lower-stage tumor and better prognosis than SNAI2-negative renal cell carcinomas. To our best knowledge, studies in human samples

have not yet addressed such relationship in anaplastic thyroid carcinoma. However, the finding of epithelial-mesenchymal transition at the invasive edge of papillary thyroid carcinoma¹⁰ and in lymph node metastases of papillary thyroid carcinoma¹⁷ indicates a link between induction of epithelial-mesenchymal transition and aggressive behavior in well-differentiated thyroid cancers. Our findings of SNAI2 and TWIST1 expression in anaplastic thyroid carcinoma, but not in well-differentiated thyroid carcinomas further suggest that this relationship probably exist in thyroid cancers as well. Signal transduction has been linked to cell proliferation, but we did not study signal transduction in the current manuscript. Integrin and its receptors have also been linked to epithelial-mesenchymal transition, but integrin was not examined in the current study.

Quantitative RT-PCR in thyroid cell lines detected the highest levels of CDH1 mRNA in the normal thyroid cell line, whereas the anaplastic thyroid carcinoma cell line had the highest levels of SNAI2 and TWIST1 mRNA and reduction of CDH1 mRNA levels relative to the normal thyroid. These findings are generally supportive of our immunohistochemical observations in primary human tissue samples.

In summary, our results support the role of epithelial-mesenchymal transition in anaplastic thyroid carcinoma development. Immunolabeling for SNAI2, TWIST1 and CDH1 may, in principle, be used as part of a panel in the differential diagnosis of anaplastic thyroid carcinoma in limited tissue specimens. However, the results should be interpreted with caution as SNAI2 and TWIST1 can be detected by immunohistochemistry in stromal and endothelial cells and also in a variety of other poorly differentiated carcinomas.

Acknowledgements

We thank Dr J Copland at the Mayo Clinic Jacksonville for the 16T and 21T cell lines, Tom Pier at the Translational Research in Pathology Lab at the UW School of Medicine for skillful construction of the thyroid tissue microarray, and Dr Bill Rehrauer for helpful conversations about TMA construction. The study was supported by NIH-RO1 CA121115 and American Cancer Society MEN2 Thyroid Cancer Professorship (HC).

Disclosure/conflict of interest

The authors declare no conflict of interest.

References

- Thiery JP, Acloque H, Huang RY, *et al*. Epithelial-mesenchymal transitions in development and disease. *Cell* 2009;139:871-890.

2 Hollier BG, Evans K, Mani SA. The epithelial-to-mesenchymal transition and cancer stem cells: a coalition against cancer therapies. *J Mammary Gland Biol Neoplasia* 2009;14:29–43.

3 Polyak K, Weinberg RA. Transitions between epithelial and mesenchymal states: acquisition of malignant and stem cell traits. *Nat Rev Cancer* 2009;9:265–273.

4 Peinado H, Olmeda D, Cano A. Snail, Zeb and bHLH factors in tumour progression: an alliance against the epithelial phenotype? *Nat Rev Cancer* 2007;7:415–428.

5 Shioiri M, Shida T, Koda K, *et al*. Slug expression is an independent prognostic parameter for poor survival in colorectal carcinoma patients. *Br J Cancer* 2006;94: 1816–1822.

6 Hotz B, Arndt M, Dullat S, *et al*. Epithelial to mesenchymal transition: expression of the regulators snail, slug, and twist in pancreatic cancer. *Clin Cancer Res* 2007;13:4769–4776.

7 Sarrio D, Rodriguez-Pinilla SM, Hardisson D, *et al*. Epithelial-mesenchymal transition in breast cancer relates to the basal-like phenotype. *Cancer Res* 2008;68: 989–997.

8 Ansieau S, Morel AP, Hinkal G, *et al*. TWISTing an embryonic transcription factor into an oncoprotein. *Oncogene* 2010;29:3173–3184.

9 Mikami S, Katsume K, Oya M, *et al*. Expression of Snail and Slug in renal cell carcinoma: E-cadherin repressor Snail is associated with cancer invasion and prognosis. *Lab Invest* 2011;91:1443–1458.

10 Vasko V, Espinosa AV, Scouten W, *et al*. Gene expression and functional evidence of epithelial-to-mesenchymal transition in papillary thyroid carcinoma invasion. *Proc Natl Acad Sci USA* 2007;104:2803–2808.

11 Kebabew E, Greenspan FS, Clark OH, *et al*. Anaplastic thyroid carcinoma. Treatment outcome and prognostic factors. *Cancer* 2005;103:1330–1335.

12 Wiseman SM, Masoudi H, Niblock P, *et al*. Derangement of the E-cadherin/catenin complex is involved in transformation of differentiated to anaplastic thyroid carcinoma. *Am J Surg* 2006;191:581–587.

13 Aratake Y, Nomura H, Kotani T, *et al*. Coexistent anaplastic and differentiated thyroid carcinoma: an immunohistochemical study. *Am J Clin Pathol* 2006;125:399–406.

14 Braun J, Hoang-Vu C, Dralle H, *et al*. Downregulation of microRNAs directs the EMT and invasive potential of anaplastic thyroid carcinomas. *Oncogene* 2010;29: 4237–4244.

15 Knauf JA, Sartor MA, Medvedovic M, *et al*. Progression of BRAF-induced thyroid cancer is associated with epithelial-mesenchymal transition requiring concomitant MAP kinase and TGFbeta signaling. *Oncogene* 2011;30:3153–3162.

16 Salerno P, Garcia-Rostan G, Piccinin S, *et al*. TWIST1 plays a pleiotropic role in determining the anaplastic thyroid cancer phenotype. *J Clin Endocrinol Metab* 2011;196:E772–E781.

17 Hardy RG, Vicente-Duenas C, Gonzalez-Herrero I, *et al*. Snail family transcription factors are implicated in thyroid carcinogenesis. *Am J Pathol* 2007;171: 1037–1046.

18 R Development Core Team R: A Language and Environment for Statistical Computing. R Foundation for Statistical Computing: Vienna, Austria, 2011.

19 Riesco-Eizaguirre G, Rodriguez I, De la Vieja A, *et al*. The BRAFV600E oncogene induces transforming growth factor beta secretion leading to sodium iodide symporter repression and increased malignancy in thyroid cancer. *Cancer Res* 2009;69:8317–8325.

20 Zito G, Richiusa P, Bommarito A, *et al*. In vitro identification and characterization of CD133(+) cancer stem-like cells in anaplastic thyroid carcinoma cell lines. *PLoS One* 2008;3:e3544.

21 Friedman S, Lu M, Schultz A, *et al*. CD133+ anaplastic thyroid cancer cells initiate tumors in immunodeficient mice and are regulated by thyrotropin. *PLoS One* 2009;4:e5395.

22 Liu J, Brown RE. Immunohistochemical detection of epithelialmesenchymal transition associated with stemness phenotype in anaplastic thyroid carcinoma. *Int J Clin Exp Pathol* 2010;3:755–762.

23 Sung CO, Lee KW, Han S, *et al*. Twist1 is up-regulated in gastric cancer-associated fibroblasts with poor clinical outcomes. *Am J Pathol* 2011;179:1827–1838.